Facies and origin of shales from the mid-Proterozoic Newland Formation, Belt Basin, Montana, USA

JUERGEN SCHIEBER

Department of Geology, The University of Texas at Arlington, Arlington, TX 76019, USA

ABSTRACT

Shales constitute more than 60% of the world's sediments, yet while facies models for sandstones and carbonates are at a high level of sophistication, the study of shales has clearly lagged behind. In the mid-Proterozoic Newland Formation six major shale facies types, deposited in nearshore to basinal environments, are distinguished on the basis of bedding characteristics, textural features, and the proportions of silt, clay and carbonate. Textural features of these shale types are related to sedimentary environments as deduced from associated lithologies. The shales are undisturbed by bioturbation, and their textural and sedimentary characteristics reflect subaqueous growth of microbial mats, erosion and deposition by storms, deposition of flocculated vs. dispersed clays, continuous slow background sedimentation, winnowing by waves or currents, and subaerial exposure.

INTRODUCTION

Owing to the fine grained nature of shales, textural features tend to be small, and usually need to be examined under higher magnification. On the other hand, the small size of features usually causes a larger variety of them to be assembled in a single hand specimen or thin section. This compensates, to some degree, for the inconveniences caused by small grain size. Even though petrographic microscopes are more readily available to geologists than any other piece of laboratory equipment, detailed microscope descriptions of shales are surprisingly rare. Notable exceptions are studies by Rubey (1931), Folk (1960, 1962), and Burger (1963). Small grain size, the difficulty of collecting outcrop samples suitable for preparation of thin sections, and the tendency of samples to disintegrate during transport and handling, are probably the main reasons why detailed microscope studies of shales are not often attempted.

Shales of the Newland Formation (Belt Supergroup) and associated sedimentary units (Figs 1 & 2) are well consolidated, unmetamorphosed and not bioturbated. They were therefore chosen for an investigation of the variability of shale facies.

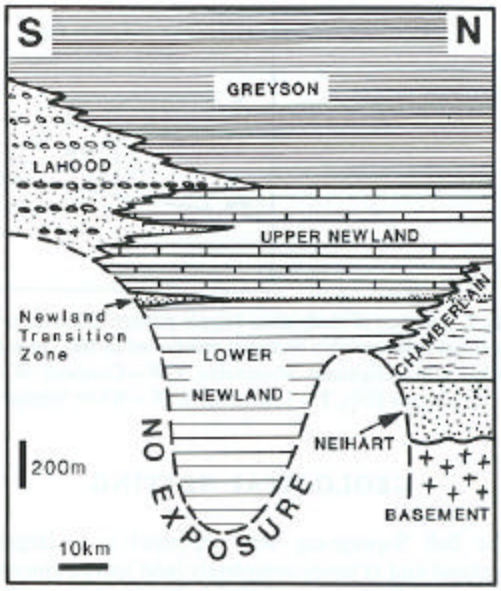

Fig. 1. Stratigraphic relationships between Newland Formation and adjacent stratigraphic units as proposed by Boyce *(1975)* and Schieber (1985)

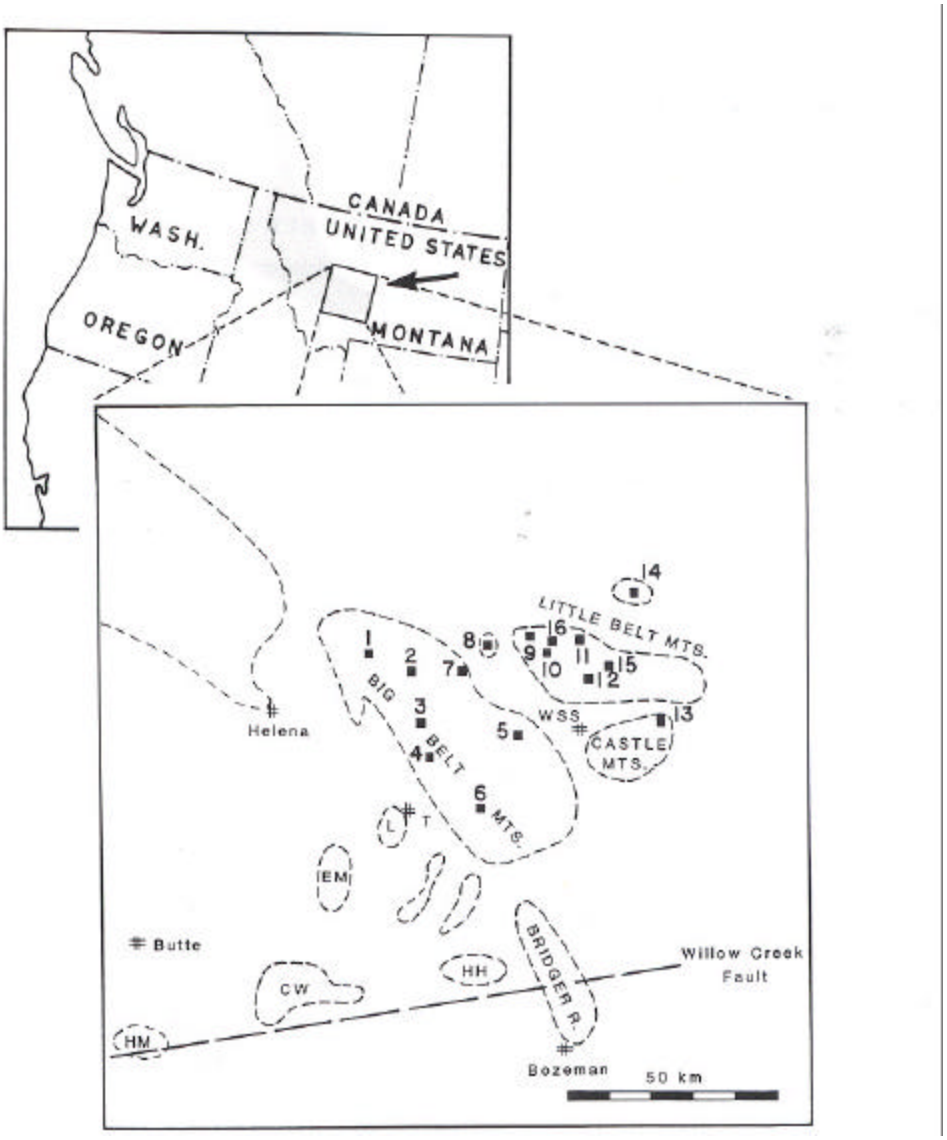

Fig. 2. Location of study area. Stipple pattern indicates present day outline of Belt Supergroup exposures. Numbers indicate localities (stratigraphic sections) mentioned in text. In enlarged portion of map, dashed lines indicate outcrop areas of Belt rocks. HM=Highland Mountains, CW=Cardwell-Whitehall area, HH=Horseshoe Hills, EM=Elkhorn Mountains, L=Limestone Hills, T=Townsend, WSS=White Sulphur Springs.

GEOLOGICAL SETTING

The Belt Supergroup was deposited in a largely enclosed and at times completely land locked epicontinental basin (Stewart, *1976),* the Belt basin, between *1450* and *650* Ma (Harrison, *1972).* The Newland Formation occurs in the so-called Helena embayment, a sub-basin of the Belt basin (Figs 1 & 2). It has been subdivided into a lower member (mainly dolomitic shales) and an upper member (interstratified packages of shales and carbonates) by Nelson *(1963).* In the transition between the lower and the upper members of the Newland Formation, beds of feldspathic sandstones are found within the shales. This

sandstone bearing interval is informally called the 'Newland transition zone' (Schieber, 1985). The Chamberlain Shale is a partial lateral equivalent of the Newland Formation along the northern margins of the Helena embayment (Schieber, 1985, 1986a). The LaHood Formation (McMannis,1963), a predominantly coarse clastic alluvial fan to deltaic sequence (Boyce, 1975), is a partial lateral equivalent along the southern margin (Boyce, 1975; see also Fig. 1). A brief overview of the sedimentary history of the Helena embayment is given in Schieber (1986a).

DESCRIPTION AND INTERPRETATION

Six shale facies types occur in outcrop in the Newland Formation and associated units. Identification is based on easily observable features such as mechanical strength, carbonate content, silt content, and sedimentary features. Information on composition, particle size, and particle shape is summarized in Table 1.

Approximately 2000 samples of shale and 500 petrographic thin sections were examined. In 50 samples the major minerals were qualitatively determined by X-ray diffraction. About 100 samples were analysed for major elements by X-ray fluorescence. The data were used to quantitatively constrain mineralogical compositions as determined from thin sections. Staining with Alizarin Red-S was used to distinguish calcite from dolomite in thin sections.

Most classification schemes for shales utilize relative amounts of clay and silt-sized particles, stratification, and state of induration as classification parameters. However, these classification schemes, though useful in some cases, are not suitable for the Newland shales. For example, if the scheme of Potter, Maynard & Pryor (1980, p. 14) is compared with the data in Table 1, it is obvious that all shale types but one would be described as dolomitic clay shales. In the case of the Newland shales, consideration of textural features allows distinction of a much larger variety of shale types.

A textural approach to shale distinction was chosen in this study, because textural features are much more closely related to conditions of sedimentation than compositional features. Because of compositional variability from bed to bed, the data in Table I are only of general nature. Facies characteristics are summarised in Fig. 3. Features of associated lithologies are compiled from Schieber (1985).

Striped shale

The characteristic striped appearance of this facies is produced by the interlayering of four rock types: carbonaceous silty shale, dolomitic clayey shale, siltstone, and lithoclast beds. This shale type has been described in detail by Schieber (1986b). Important textural features are shown in Figs 4 & 5, and summarised in Fig. 3. Most siltstone beds, showing parallel lamination, cross-lamination, and graded rhythmites (Reineck&Singh, 1972), are in gradational contact with overlying beds of dolomitic clayey shale, thus forming silt/mud couplets (Figs 4 & 5). Lithoclast beds (< 50 mm thick), if present, are usually overlain by silt/mud couplets, thus forming clast/silt/mud triplets. Thicker lithoclast beds have erosive bases and form lenticular channel fills.

Beds of medium to coarse grained sandstone (as much as 400 mm thick) with sharp undulating bases and hummocky cross-stratification (Harms *et al.*, 1975) occur within the striped shale facies. Interstratified carbonate units contain current ripples, wave ripples, cryptalgal laminites and flat pebble conglomerates.

Interpretation

Schieber (1986b) interpreted carbonaceous silty shale beds as fossilized microbial mats on the basis of irregular wavy-crinkly laminae, false cross-lamination (Schieber, 1986b, p. 529), and mechanical strength during soft sediment deformation. Silt/mud couplets and clast/silt/mud triplets were interpreted as storm deposits, because of the close resemblance to storm deposits of modern muddy shelf seas and because of the presence of interbedded hummocky cross-stratified sandstones (Aigner & Reineck, 1982; Dott & Bourgeois, 1982). The sandstones probably represent only very exceptional major storms, whereas silt/mud couplets and clast/silt/mud triplets were the result of more frequent, average intensity storms (Schieber, 1986b, 1987).

Presence of storm deposits and absence of any signs of emergence suggests that the striped shale facies accumulated between fair weather and average storm wave base. It is envisaged that subaqueous flat microbial mats colonized the sediment during periods of low sediment supply, and that storms mobilized mud in marginal areas and spread it out over the microbial mats (deposition of silt/mud couplets). After the settling of storm layers microbial mats recolonized the sediment surface. Smaller pulses of sediment, caused, for example,

Table 1. Petrographic summary of shales

	Silty shale	**Carbonaceous swirl shale**	**Striped shale**
Clay	20-90% (ill., kaol., ±chlorite)	30-50% (illite, ±kaolinite)	LO-70% (illite, ±kaolinite)
Silt	5-60% (qtz., tr. fldsp.), 0.02-0-1 mm, a. -s.a.	1-5%, (qtz.) 0-02-0.1 mm, a.-s.a.	1-30% (qtz., dolos., tr. fldsp.) 0~02OV mm, a.-s.a.
Dolomite	None	0-40%, 3-20 gym, irr.-rhombic	0-50%, 3-20 wm, irr.-rhombic
Calcite		Tr.	Tr.
Sand	Only in intercalated beds	None	Only in intercalated sandst. beds
Micas	1-10% (must., ±biot.), 003-0~5 mm, flakes	2-5% (muse, ±biot.) 003 05 mm, flakes	Tr. -2% (muse, ±biot.) 0~030~5 mm, flakes
Heavy minerals	Tr. zircon & tourmaline, 002-0~ 1 mm, s. r.-r.	Tr. zircon, tourmaline, 00201 mm, s.r.-r.	Tr. zircon, tourmaline, 0~020~1 mm, s.r.-r.
Pyrite	Tr., 5-20 μm	0-1 %, 5-20 μm, cubes and framboids (0 1-05 mm)	I-5%, 5-20 μm, cubes and framboids (0~ 1 W 5 mm)
Debris	None	Up to 2% carb. fragm., 005 20mm,shale fragm., up to 20 mm	Up to 1 % carb. fragm., 005-1 mm, shale, siltst., and dolost. fragm., up to 20 mm
Bedding	Wavy-parallel, 1-50 mm	Uneven, nonparallel, 1-10 mm	Parallel, 1 mm to several cm
Fissil.	Good	Moderate to poor	Good

	Carbonaceous streak shale	**Gray dolomitic shale**	**Calcareous silty shale**
Clay	15-70% (illite)	15-35% (illite, ±kaolinite) 0-5% (qtz., dolos., O~O1W05 mm, a.-s.a.; peloids, 0~05-0-1 mm) 15-50%, 3-20 μm, irr.-rhombic	20-40% (illite, ±kaolinite)
Silt	5-20% (qtz., tr. fldsp.), 002-0~ 1 mm, a.-s.a.		2-10% (qtz., calcis.. & dolos.) 0~020~1 mm, a.-s.a.
Dolomite	0-40%, 3-20 μm, max. 50 μm. irr. rhombic		5-15%, 3-20 gm. irr.-rhombic
Calcite	Tr.-few %, same app. as dolomite	Tr.-few %, same app. as dolomite	5-15%, 10-100 wm, irr.
Sand	0-30% (qtz., fldsp., carb. part., met. r.-fr.), 025-15 mm, s.r.-r.	None	Only in scattered lenses
Micas	Tr.-2% (must., ±biot.) 003-2 mm, flakes	0-1% (musc., ±biot.) 0~02OM mm, flakes	Tr.-1%(musc., ±biot.)0~020~2 mm
Heavy minerals	Tr. zircon & tourmaline, 002-0 1 mm, s. r.-r.	None identified	None identified
Pyrite	0-2%, 5-20 μm, cubes	0-1 %, 5-20 pm, cubes (in places up to 10 mm) Up to 1% carb. fragm. 005-3 mm	Tr., 5-20 μm, cubes
Debris	Up to 5% carb. fragm. (005-3 mm), 0-5% shale fragm. (0~5-3 mm)		Carbonate & shale fragm., 0~ 10~4 mm; carb. fragm., 0~05Smm
Bedding	Even, parallel, 003-020 m	Even, parallel, 1-35 mm	Parallel-wavy, 0~ 1-10 mm
Fissil	Along bedding planes only	Good	Good

Abbreviations: ill. =illite, kaol.=kaolinite, qtz.=quartz, tr.=trace, fldsp.=feldspar, dolos.=dolosiltite, calcis.=calcisiltite, a.=angular, s.a.=subangular, r.=rounded, s.r.=subrounded, irr.=irregular, muse =muscovite, biot.=biotite, siltst.=siltstone, dolost.=dolostone, carb. fragm.=carbonaceous fragments, carb. part.=carbonate particles, met. r.fr.=metamorphic rock fragments, fissil.=fissility.

by floods, may have led to the deposition of shale drapes within the microbial mat beds. Recurring deposition of storm layers on microbial mats created the intimate interlayering of lithologies and the striped appearance of this fades.

Carbonaceous swirl shale

This facies is of great compositional variability (Table 1) and consists primarily of a clay-dolomite matrix with scattered quartz silt, micas, minor amounts of other minerals, and variable amounts of carbonaceous flakes (Table 1). A substantial portion (10-40%) of this shale type consists of diagenetic silica that was deposited interstitially between clay and carbonate minerals.

Compared with dolomitic clayey shale beds (striped shale fades, Fig. 5), clay minerals are not as well aligned parallel to bedding, and of the mica flakes a considerable proportion (;z~ 20%) is far out of alignment (Figs 6 & 7). Irregularly shaped carbonaceous flakes appear wavy deformed, overfolded, crumbled and rolled up in cuts perpendicular to bedding (Figs 8 & 9A). In places continuous carbonaceous films and laminae of carbonaceous silty shale (0~2-2 mm thick) occur, and may be overlain by layers and lenses of silt (1-2mm

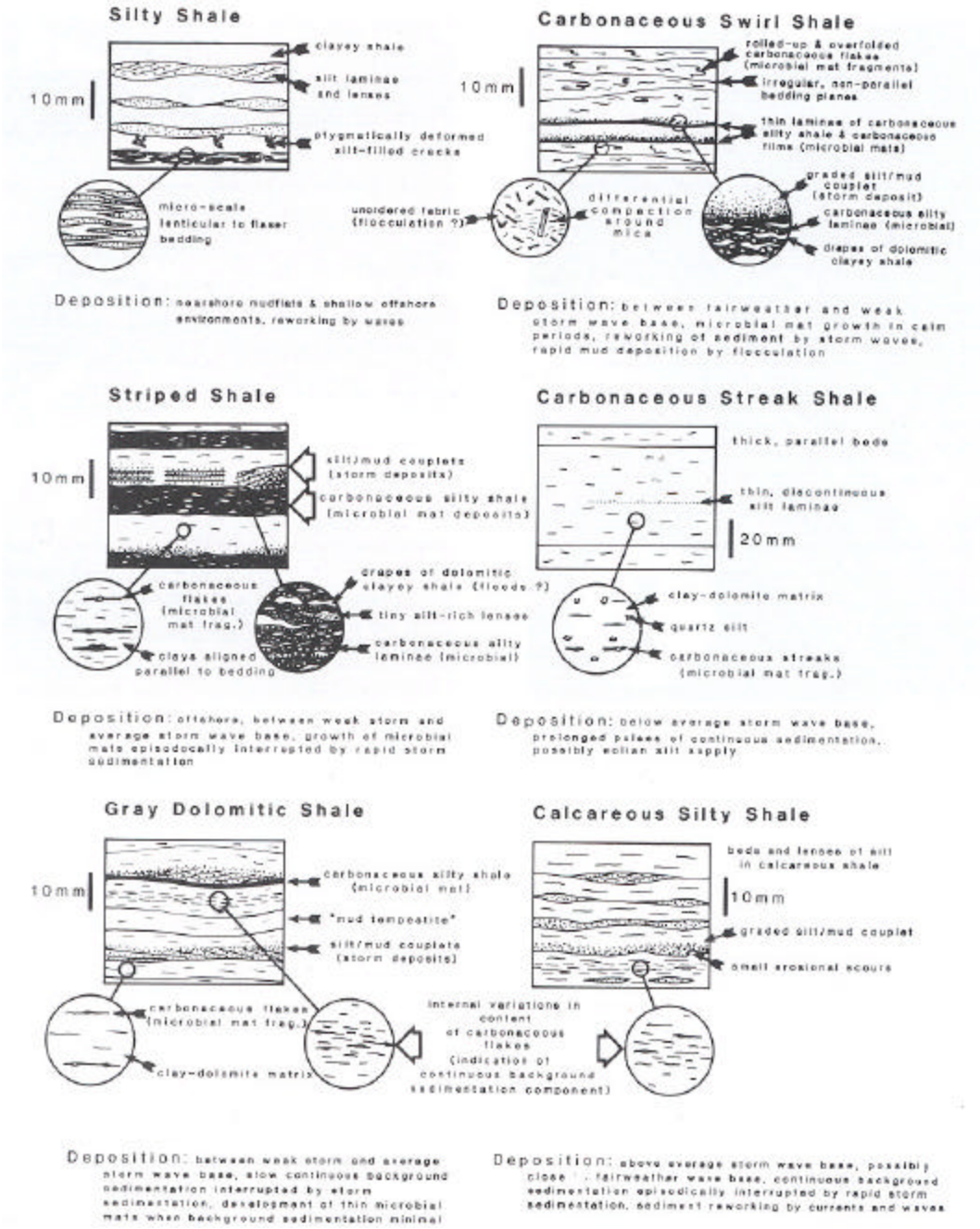

Fig. 3. Summary of shale fades features and envisaged depositional setting. The term `weak storm wave base' is used here to indicate a water depth below fair weather wave base and above average storm wave base, mainly to emphasize that the striped shale and gray dolomitic shale fades were probably deposited at somewhat greater depth than the carbonaceous swirl shale fades.

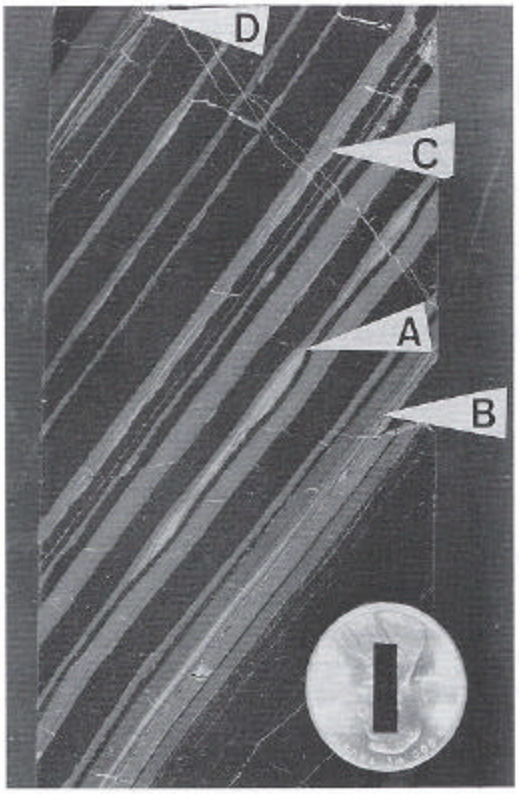

Fig. 4. Drill core specimen of striped shale. Shows silt/mud couplets (light gray) alternating with beds of carbonaceous silty shale (dark). Note cross-laminated silt lenses (arrow A), parallel laminated silt (arrow B), and graded rhythmites (arrows C and D). Coin is 19 mm in diameter, scale bar is 10 mm long.

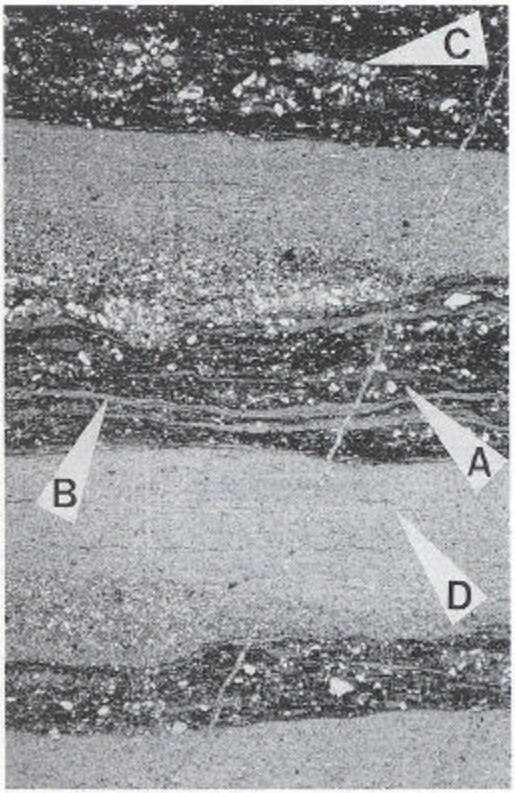

Fig. 5. Photomicrograph of striped shale which shows several beds of carbonaceous shale alternating with graded silt/mud couplets. Arrow A points out wavy-crinkly carbonaceous silty laminae that contain carbonaceous matter, clay minerals, tiny pyrite crystals, and scattered silt grains. Arrow B points out drapes of dolomitic clayey shale in carbonaceous silty shale; arrow C points out tiny silt rich lenses; arrow D points out tiny carbonaceous flakes in dolomitic clayey shale. Note the sharp contacts between carbonaceous silty shale beds and silt/mud couplets. Dolomitic clayey shale beds show preferred extinction parallel to bedding because of aligned clay minerals. Photo is 3.7 mm high.

thick) with slight grading on top (Fig. 913) and small load casts at the bottom. Nonparallel and slightly undulose bedding planes and colour banding (variable amounts of carbonaceous flakes) are a typical feature of these shales (Figs 9C & 9D). Small scale soft sediment deformation is relatively common (Fig. 9C). In a few samples small deformed shrinkage cracks were found (Fig. 9C). Shale intraclasts (< 20 mm in size) occur within shale beds. Siltstone beds (30-80 mm thick) in this fades show flaser bedding, wavy bedding, internal cross-lamination, load structures, and scour and fill structures at the base.

Packages of carbonaceous swirl shale (4-40 m thick) are intercalated with packages of fine crystalline dolostone (2-20 m thick), containing wavy-crinkly carbonaceous laminae, polygonal and incomplete shrinkage cracks, cross-laminated dolosiltite beds, erosion surfaces, scour and fill structures, and edgewise conglomerates.

Interpretation

Shrinkage cracks in these dolostones resemble those of Permian intertidal dolomites of Texas (Lucia, 1972) and of modern dolomites in ephemeral lagoons (Von der Borch, 1976). Other sedimentary features of these dolostones also suggest deposition in restricted shallow shelf lagoons with periodic emergence and sediment reworking by storms (Wilson, 1975). Sedimentary structures in siltstone beds indicate conditions of current or wave action alternating with slack water (Reineck & Singly 1980, p. 115).

Variably deformed carbonaceous flakes (or `swirls') are the outstanding textural feature of the carbonaceous

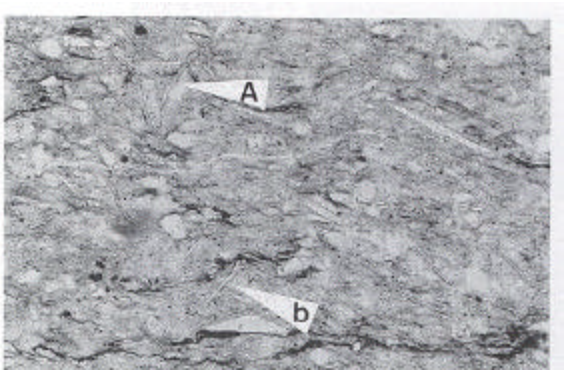

Fig. 6. Randomly oriented mica flakes in carbonaceous swirl shale. Note that a fair number of flakes are oriented in near vertical position and may show deformation due to compaction (arrows A and B). Photo is 075 mm wide.

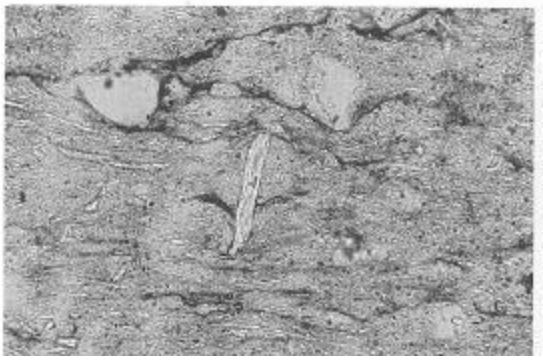

Fig. 7. Vertical standing mica flake in carbonaceous swirl shale, shows differential compaction of shale to the left and right of rigidly behaving mica. Photo is 037 mm wide.

swirl shales and were interpreted as microbial mat fragments by Horodyski *(1980).* The considerable cohesive strength of these flakes during transport and deposition, as indicated by rolled up and folded-over flakes, supports this interpretation. Thin laminae of carbonaceous silty shale and carbonaceous films in these shales are interpreted as microbial mats by analogy with the striped shale fades. They were the likely source of carbonaceous flakes. Microbial mat growth implies periods of slow deposition that allowed colonization of the sediment interface, whereas the presence of carbonaceous flakes testifies to erosion and destruction of these mats. Mat erosion and shale intraclasts indicate currents of considerable strength during erosion events (Neumann et al., *1970;* Sundborg, *1967).* The observation that carbonaceous silty shale beds are very thin and

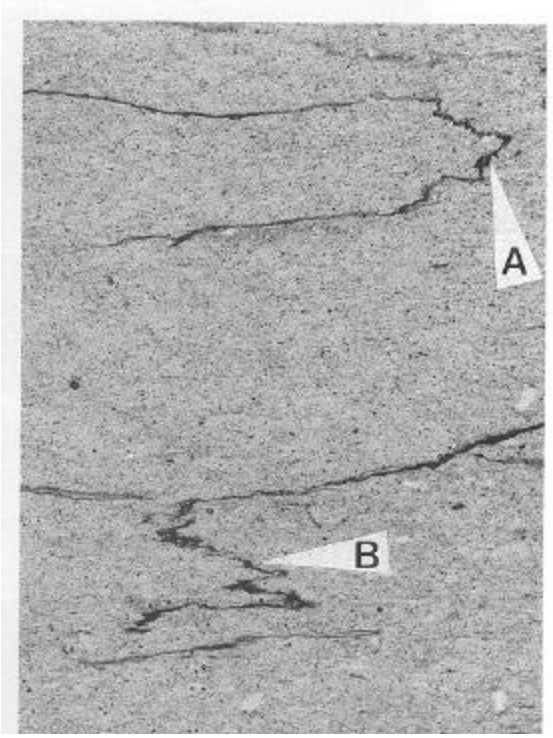

Fig. 8. Photomicrograph of deformed carbonaceous flakes in carbonaceous swirl shale. Shows folding over of carbonaceous fragment (arrow A), and flake that is `crumbled' perpendicular to bedding because of compaction (arrow B). Photo is 075 mm

much less abundant when compared with the striped shale fades (Table 1), indicates that microbial mats had only relatively short time intervals available for undisturbed growth.

The homogeneously mixed and random texture of the carbonaceous swirl shales (Figs *6 & 7)* could be due to flocculation. Experimentally flocculated muds show random orientation of clay flakes, whereas settling of dispersed clays leads to parallel alignment (Mattiat, *1969).* According to O'Brien *(1970, 1980, 1981),* the random fabric of ancient flocculated clays may still be preserved after burial and consolidation. The potential importance of flocculation in the deposition of carbonaceous swirl shales is indicated by imperfect clay mineral alignment, the abundance of disaligned and bedding-perpendicular micas (Figs *6 & 7),* and the comparatively poor fissility of these shales (O'Brien, *1970).* Obliteration of the flocculated structure during burial and compaction may have

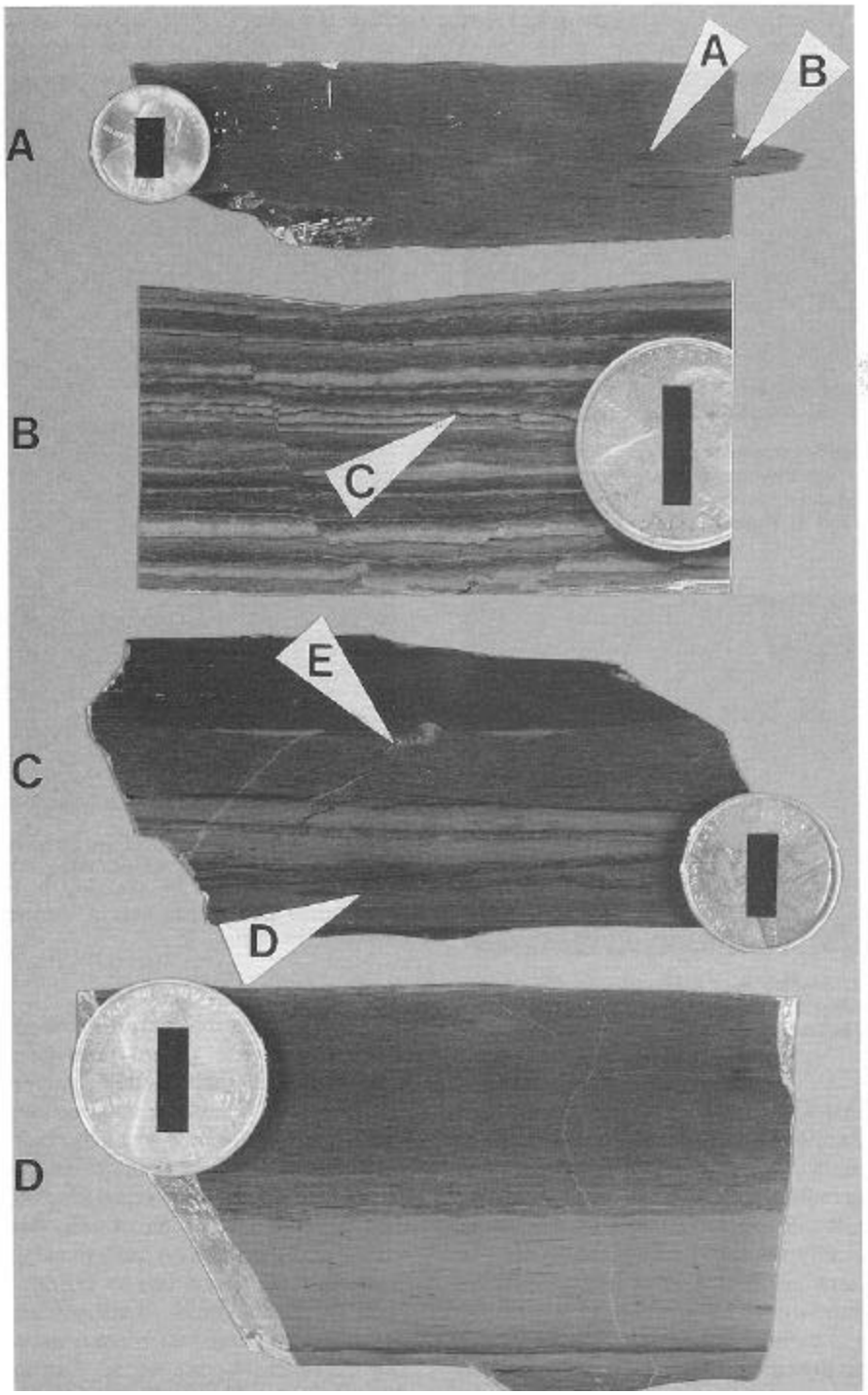

Fig. 9. Several photos of hand specimens of carbonaceous swirl shale. (A) carbonaceous swirl shale with visible `swirls' (arrows A and B); (B) specimen with abundant top-graded silt bedsand thin carbonaceous films (arrow C); (C) non-parallel, divergent bedding planes, soft sediment deformation (arrow D) and deformed, silt filled crack (arrow E); (D) colour banding in carbonaceous swirl shale, caused by variable amounts of carbonaceous flakes. Coin is 19 mm in diameter, bar scale is 10 mm long.

been prevented by diagenetic silica deposition between clays.

Deposition of recent muds can occur at fairly strong current or wave activity (McCave, 1970, 1971) at large suspended sediment concentrations. Widespread storm deposits in the Newland Formation (Schieber, 1986b) suggest mud deposition from storm-induced suspensions. Irregular bedding planes and deformed carbonaceous flakes may have formed as mud was deposited from moving waters. Frequent storm erosion suggests deposition in considerably shallower water than indicated for the striped shale facies.

Sedimentary features in these shales and in associated lithologies suggest that they probably accumulated in fairly shallow water (between fair weather and weak storm wave base). Microbial mats colonized the sediment surface in calm periods and were eroded during storms. As storms abated, rapid flocculation from moving water led to irregularly bedded muds with variably deformed microbial mat fragments. Shrinkage cracks in this facies lack any recognizable crack patterns on bedding planes and probably formed during synaeresis or early soft sediment deformation, rather than during subaereal exposure.

Carbonaceous streak shale

These shales consist of silt and carbonaceous particles that are randomly distributed in a clay-dolomite matrix (Fig. 10), and show a continuous compositional spectrum from clay to dolomite dominated varieties (Table 1). Carbonaceous particles are aligned subparallel to bedding and may impart a faint laminated character to

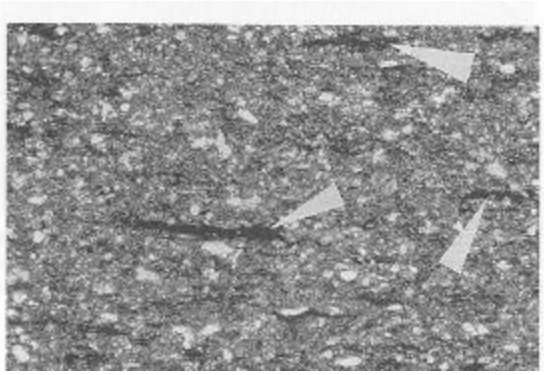

Fig. 10. Photomicrograph of typical carbonaceous streak shale. Carbonaceous flakes (arrows) float in a matrix of clay, fine crystalline dolomite, and silt. Alignment of carbonaceous fragments indicates bedding plane orientation. Photo is 1-4 mm wide.

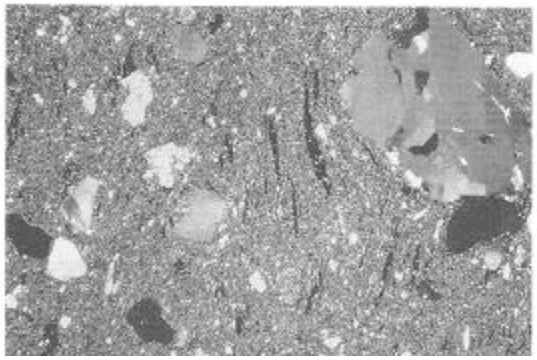

Fig. 11. Photomicrograph of carbonaceous streak shale with scattered sand grains. Carbonaceous flakes were bent around large polycrystalline quartz grain during compaction (lower right corner). Photo is 3-7 mm wide.

the rock. They appear as irregular flakes in cuts parallel to bedding, and as wavy-crinkly streaks in cuts perpendicular to bedding. Some shale beds contain up to 30% of randomly scattered sand (Fig. 1 I), consisting of rounded to subrounded quartz grains (0-25-1-5 mm), feldspar, micas, metamorphic rock fragments (0-25-1 mm), carbonate rock fragments (0-25-1-5 mm), oolites, and shale fragments (0-25-1-5 mm). In a few samples isolated, discontinuous silty laminae (< 1 mm thick) were found. Variations in carbonaceous flake concentration may cause gray indistinct cm-thick colour banding of shales. Sandstone beds (< 550 mm thick) that occur in this facies have sharp, undulate bases, may show flute casts and gutter casts, hummocky cross-stratification, and parallel lamination.

Interpretation

Lack of sedimentary structures makes this facies the most problematic one to interpret. The carbonaceous flakes are essentially identical to those in already described facies types and are considered microbial mat fragments. They were probably swept in from other areas, because no evidence of *in* situ mat growth is found. Evidence of erosion and sediment reworking is absent in this facies, except at the base of hummocky cross-stratified sandstones. Because the latter were probably deposited during exceptionally strong storms (Schieber, 1987), shale deposition most likely occurred below average storm wave base.

Lack of sorting within shale beds could imply continuous rapid sedimentation from suspension (Potter *et al.*, 1980, p. 22) and absence of reworking by bottom

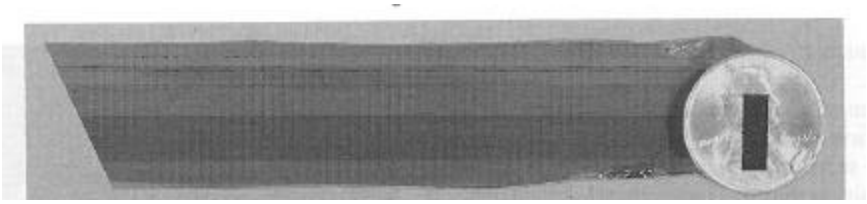

Fig. 12. Colour banding in hand specimen of gray dolomitic shale. Coin is 19 mm in diameter, scale bar is 10 mm long.

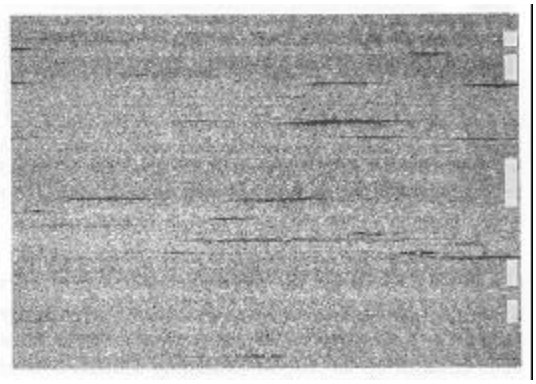

Fig. 13. Photomicrograph of gray dolomitic shale. Shows faint internal banding due to variations in dolomite content. Laminae with higher dolomite content appear lighter than those with lower dolomite content (indicated by bars). Note also the horizontally aligned carbonaceous flakes. Photo is 3.7 mm wide.

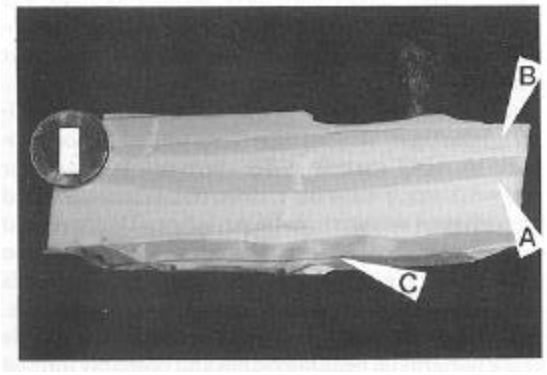

Fig. 15. Silt/mud couplets with low angle cross-lamination in gray dolomitic shale. Note sharp bases and gradational top portions (arrows A and B) of the wavy silt beds. Arrow C points out a thin bed of carbonaceous silty shale. Coin is 19 mm in diameter, scale bar is 10 mm long.

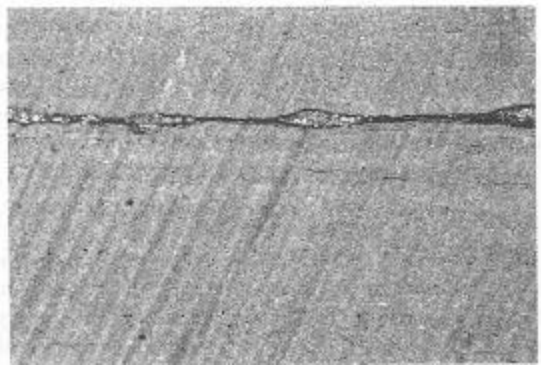

Fig. 14. Photomicrograph of carbonaceous film in gray dolomitic shale. Photo is 3-7 mm wide.

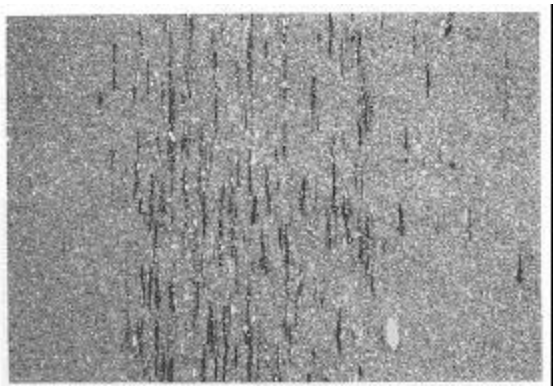

Fig. 16. Gradual variation in the content of carbonaceous flakes in gray dolomitic shale. This may indicate gradual changes in sedimentation rate and more or less continuous background sedimentation. Area in photo is 3-7 mm wide.

currents. Massive bedding of shales (Table 1) implies that there were successive prolonged pulses of continuous sedimentation, rather than continous sedimentation throughout. Minor fluctuations in sediment supply are indicated by carbonaceous flake content variations (colour banding). Thin discontinuous silt laminae within shale beds indicate infrequent sediment reworking by weak bottom currents. Randomly scattered silt grains in this facies could be of aeolian origin, similar to silt introduced into the North Atlantic by Saharan dust storms (Windom, 1975). Such a `rain' of aeolian silt, superimposed on offshore deposition of clay,

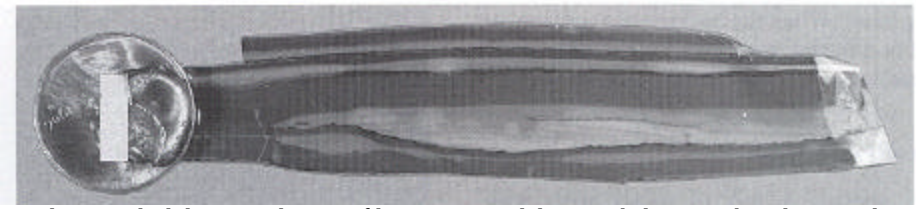

Fig. 17. Cross-laminated silt lenses and trains of lenses in gray dolomitic shale. Note sharp lower and gradational upper boundary of silt beds. Coin is 19 mm in diameter, scale bar is 10 mm long.

carbonate mud, and carbonaceous flakes could have led to randomly scattered silt in a clay/carbonate matrix.

A remaining problem is the interpretation of those rare shale beds that contain up to *30%* randomly scattered sand grains. That the components of these beds simply settled from suspension is highly unlikely because the relatively large water depth (deposition below average wave base) demands size segregation of particles during settling. The textural resemblance of these beds to pebbly mudstones (albeit on a different scale) suggests a gravity flow origin (Middleton & Hampton, *1976).* Because the sand grains are identical to those in the interbedded storm sands, one might speculate that loading of bottom muds by storm sands led to gravity flow and sand/mud mixing in areas of sufficient slope.

Gray dolomitic shale

This facies consists essentially of three rock types, dolomitic clayey shale (constitutes *x90-95%* of facies), siltstone (consisting of dolosiltite, quartz, dolomitic peloids), and carbonaceous silty shale. Beds of the latter are of the same appearance as in the striped shale facies, but are rare and usually very thin (< 1 mm, rarely in excess of *5* mm).

Boundaries of dolomitic clayey shale beds are marked by variations in colour (Fig. *12),* dolomite/ clay ratio (Fig. *13),* by carbonaceous films or thin beds of carbonaceous silty shale (Fig. *14, 15),* and by silt beds (Fig. *15).* Thicker layers of dolomitic clayey shale show internal gradual variations in the content of carbonaceous flakes (Fig. *16).* Silt occurs as thin laminae (<1 mm thick), as lensy-wavy beds (< *20* mm thick, Fig. *15),* or as trains of lenses and crosslaminated ripples (Fig. *17).* Silt beds commonly form silt/mud couplets with overlying shale beds (Fig. *15),* have non-erosive basal contacts, and show the same sedimentary features as silt beds in the striped shale facies. In places silt ripples with sharp tops occur, as well as composite silt beds that consist of overriding ripples with variable and opposing dips of foresets.

Interpretation

A striking similarity to the striped shales exists with respect to silt/mud couplets (analogously interpreted as storm deposits), whereas the paucity of carbonaceous silty shale beds (likewise considered fossil microbial mats) is the most notable contrast to the striped shales. Although a large portion of shale beds has at least some silt at the bottom, a considerable portion lacks silt at the bottom and has sharp top and bottom contacts (Fig. *12).* These latter shale beds probably can be considered very distal storm layers, akin to `mud tempestites' in recent storm deposits (Aigner & Reineck, *1982).* Wave action may have produced the composite silt beds (Reineck & Singh, *1980, p. 103)* and may indicate that storm waves at times reached the sea floor.

Paucity of carbonaceous silty shale beds in this facies may be due to large sedimentation rates or insufficient light penetration, preventing establishment and growth of microbial mats. However, modern microbial mats can prosper at fairly large sedimentation rates (Gebelein, *1969;* Gerdes et al., *1985).* Light penetration is affected by turbidity and water depth (Brock, *1976),* but water depth was probably not a decisive factor, because interbedding of striped and gray dolomitic shales indicates similar water depth for both facies. Internal gradual variations in the content of carbonaceous flakes (Fig. *16)* indicate continuous background sedimentation during deposition of gray dolomitic shales. Increased turbidity and light attenuation by this background component might well have caused paucity and thinness of microbial mat deposits in gray dolomitic shales.

To summarise, deposition of gray dolomitic shales had an episodic (storm deposits) and a more or less continuous (background sedimentation) component, and occurred in an offshore setting below fair weather wave base (probably between weak storm and average storm

wave base). When the background component was absent or minimal, microbial mats colonized the sediment surface.

Calcareous silty shale

This facies consists mainly of clayey shale with variable amounts (Table 1) of dolomite, calcite, quartz silt, carbonaceous flakes (parallel to subparallel to bedding), and carbonate and shale fragments. In a few samples continuous carbonaceous films occur. Boundaries between individual shale beds are marked by the same features as noted from the gray dolomitic shales. Internal gradual variations in the content of carbonaceous flakes occur in thicker shale beds. Silt occurs as thin laminae (< 1 mm thick; Figs 18 & 19), as lensy-wavy beds (< 5 mm thick), or as trains of lenses and cross-laminated ripples. Upper and lower boundaries of silt beds and ripples are usually sharp, but top-grading (silt/mud couplets) and graded rhythmites were also observed. Small scours occur at the base of silt beds (Fig. 18). Cross-laminated lenses of medium to coarse sand (< 20 mm thick) with erosive bottom contacts also occur.

Calcareous silty shales underlie, overlie, and are interbedded with limestones that contain beds of siltstone, medium to coarse sandstone, and flat pebble conglomerates (pebble size up to 15 cm). Silt and sand lenses are cross-laminated (asymmetrical ripples) and may form beds of overriding ripples. Silt ripples may show typical wave-produced features, such as formdiscordant internal structure, intricately interwoven cross-lamination, and cross-stratal off shoots (Reineck & Singly 1980, p. 103). Sandstone beds show planar cross-bedding as well as symmetrical ripples with spill-over aprons (Seilacher, 1982, p. 338). Clast supported, locally imbricated flat pebble conglomerates occur in erosive channels (as much as 2 m wide and 0.5 m deep).

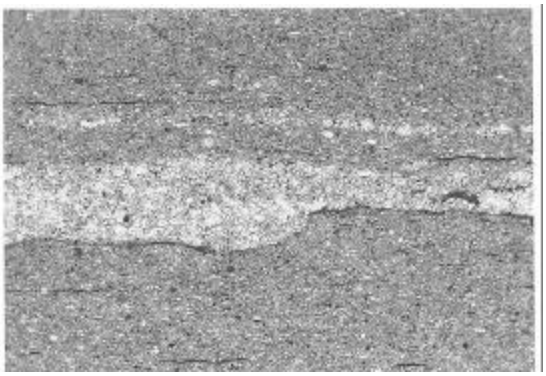

Fig. 18. Silt bed in calcareous silty shale with gradational upper contact and small scours at the base. Area in photo is 3.7 mm wide.

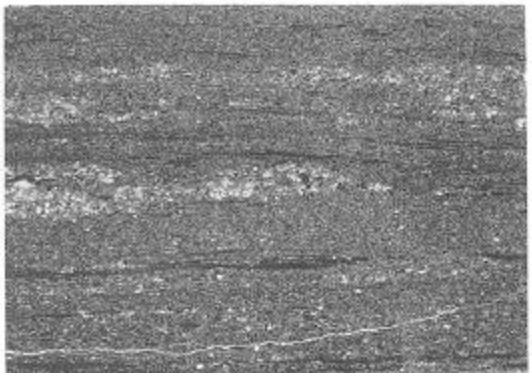

Fig. 19. Silt lenses and large carbonaceous flakes in calcareous silty shale. Area in photo is 3.7 mm wide.

Interpretation

Sedimentary features in associated carbonates indicate strong episodic currents, sediment reworking by currents and waves, and probably fairly shallow water at the site of deposition. At least part of the waveformed ripples originated during storms (symmetrical ripples with spill-over aprons; Seilacher, 1982, p. 338).

Graded rhythmites and silt/mud couplets indicate episodic shale deposition, and absence of microbial mat deposits (except carbonaceous films) is probably due to frequent reworking and continuous background sedimentation (variable content of carbonaceous flakes). Erosion surfaces indicate intermittent strong currents which may also have reworked storm layers into silt beds and lenses with sharp upper surfaces. Calcareous silty shales differ from the similar looking gray dolomitic shales with respect to microbial mat deposits (absent) and erosional features (common), and were probably deposited above average storm wave base and close to fair weather wave base.

Silty shale

This fades consists mainly of silty shales and interbedded siltstones. The silty shales are composed of alternating laminae (0.2-3 mm thick) of silt (greenish gray) and clayey shale (dark gray). Silt laminae (60% quartz silt, 1-2% mica flakes, traces of tourmaline and zircon) are usually wavy (pinch and swell) or consist

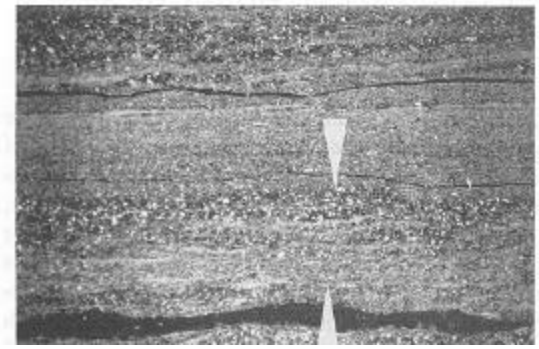

Fig. 20. Micro-flaser bedding in silty shale (between arrows). Area in photo is 10 mm wide.

of individual silt lenses. They may show internal low-angle cross-lamination, and load casts and scours at the bottom. Micro-scale lenticular to flaser bedding (Fig. 20), consisting of tiny silt lenses (only a few grains thick) interwoven with thin clay drapes, is also present. Clayey shale laminae contain 5-20% silt of smaller average size than the silt in the silt laminae, 5-10% mica flakes, and clays (illite). Contacts between silt and clay beds are usually sharp (Fig. 21). In places ptygmatically deformed, silt-filled cracks occur.

Siltstone beds (5-50 mm thick) are compositionally identical to the silt laminae and occur mainly as cross-laminated wavy beds and lenses. They may contain mudcracks, clay galls, load-casted ripples (Reineck & Singh, 1980, p. 86), and may fill erosional rills cut into silty shale.

Laterally discontinuous sandstone packages (0-33 m thick) with beds of very fine to very coarse grain size are associated with silty shales and contain them as a subordinate facies. Quartz pebble conglomerate beds (< 50 mm thick) occur in the sandstone packages. Sedimentary structures include cross-lamination, parallel lamination, wavy bedding, wave ripples, intricately interwoven cross-lamination (Reineck & Singh, 1980, p. 103), evenly laminated sand with low-angle truncation surfaces (sets 1-6 cm thick), erosive channels, and mud cracks. The sandstones may also contain abundant clay galls in certain beds.

Interpretation

Deposition in fairly shallow water is suggested by sedimentary features in associated sandstones, indicating occasional presence of very strong currents, wave reworking, periods of subaerial exposure, and shoaling waves (evenly laminated sand with low angle truncation surfaces). Alternation of wavy and lenticular silt laminae with clay laminae is often thought to be the product of alternating current and slack water conditions on tidal mudflats (Reineck & Singh, 1980, p. 115). Micro-scale lenticular to flaser bedding, indicating pulsations in current flow in such a setting (Reineck & Wunderlich, 1969), as well as wavy to lenticular bedding and

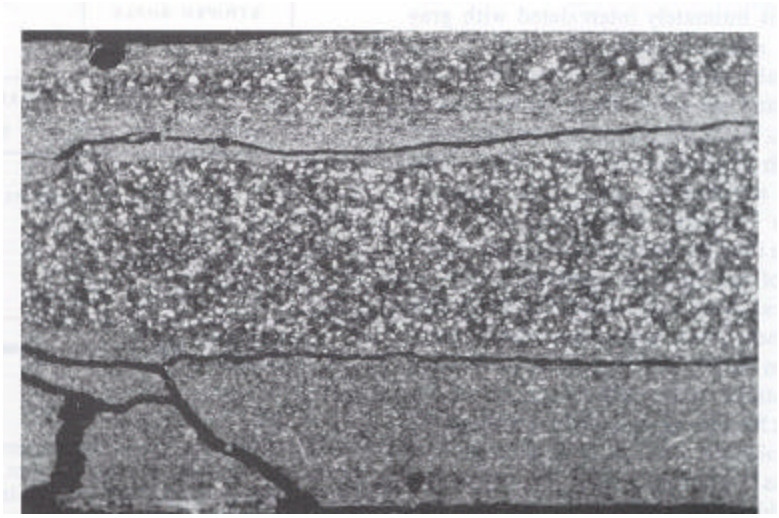

Fig. 21. Alternating clayey shale and siltstone beds in silty shale. Area in photo is 10 mm wide.

mudcracks (siltstone beds), would be compatible with an intertidal interpretation. However, because the Helena embayment was part of an isolated epicontinental basin (Stewart, 1976), tidal currents were most likely minor or absent. Wavy and lenticular bedding can also be produced by intermittent wave action (Reineck & Singh, 1980, p. 115), and because abundant evidence of wave action is found in the associated sandstones, it is envisaged that the silty shales accumulated in a nearshore setting, in which winnowing by waves produced alternating silt and clay laminae. Evidence of intermittent exposure (mudcracks) suggests accumulation on mudflats and in very shallow offshore environments.

INTERBEDDING OF FACIES TYPES AND LATERAL RELATIONSHIPS

Logging of drill cores from the Newland Formation showed that its various shale facies can be very intimately interbedded. Smooth transitions between facies packages (from 10 cm to tens of metres thick) are the rule, and facies intercalation can be demonstrated in outcrop. However, whereas some facies types are found intercalated quite commonly, others are rarely or never in contact with each other. Some facies associations occur over large portions of the outcrop area, but others are restricted to certain areas.

The striped shale facies is dominant in the shale packages of the upper member of the Newland Formation and is intimately intercalated with gray dolomitic shale and calcareous silty shale in the transition zones above and below carbonate horizons. In the northern and southern portions of the Helena embayment (Fig. 2) the striped shales are also found intercalated with carbonaceous swirl shales. Gray dolomitic shales are strongly dominant in the lower member of the Newland Formation, and occur interbedded with thin intervals of striped shale. In the upper member of the Newland Formation they are associated with calcareous silty shale in shale/carbonate transition zones. Intervals of calcareous silty shale may also contain beds of carbonaceous swirl shale. Carbonaceous streak shales occur mainly in the southern Big Belt Mountains, interbedded with striped shale and gray dolomitic shale. Silty shales occur only along the margins of the Helena embayment, and may contain interbedded carbonaceous swirl shale. Observed shale facies interrelationships are summarized in Fig. 22.

A CONCEPTUAL MODEL OF SHALE SEDIMENTATION IN THE NEWLAND FORMATION

As shown above, differences in shale fades can be related to different depositional settings. Absence of unconformities and smooth and regular facies transitions indicate that Walther's Law of Facies (Walther, 1894) should apply. Any depositional model for these shales should have as variables two simultaneous sediment sources (carbonate and terrigenous), episodic vs. continuous sedimentation, and water depth (implying energy level of environment). Figure 22 shows a simple sedimentation model in which facies are arranged by water depth. Semi-arid climate (Schieber, 1985) probably caused episodic terrigenous sedimentation and more or less continuous carbonate production in carbonate environments (evidence for continuous background sedimentation only found in carbonate-rich facies types).

Testing the model in Fig. 22 is subject to limitations, because of discontinuous outcrops, the erosional remnant

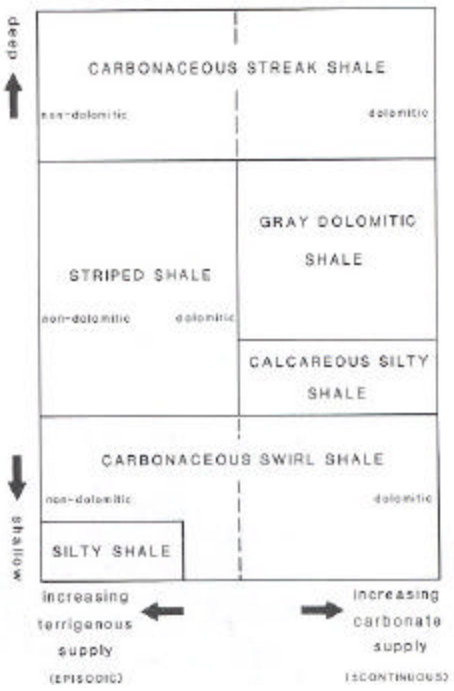

Fig. 22. Hypothetical fades arrangement along a shoreline to basin centre transect according to apparent depth of deposition and energy level of the envisioned environment. Two types of sediment supply (terrigenous vs carbonate), and continuous vs. episodic sedimentation are taken into consideration.

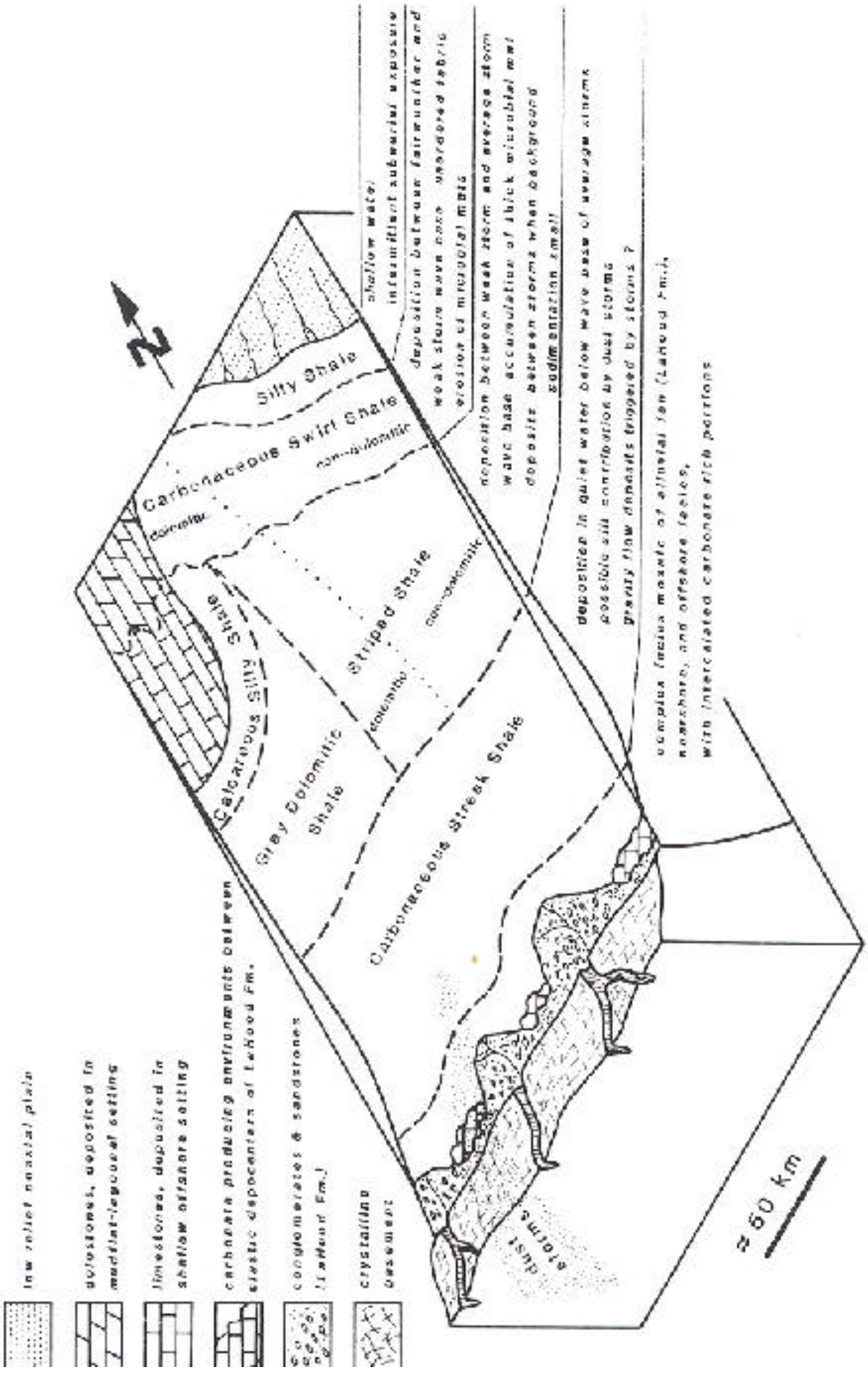

Fig. 23. A N-S slice through the Helena embayment (modified from Schieber, 1985) and a summary of my view of shale facies associations, sediment sources, and sedimentary processes.

character of the Helena embayment, and correlation problems in the southern part of the embayment (Figs 1 & 2). However, consistency with present knowledge can be tested despite these limitations. Because the basin was probably an E-W trending half-graben with a gentle flexure along the northern margin during deposition of Newland transition zone and upper member of the Newland Formation (Schieber, 1985), one should expect to go from shallower to deeper environments along a N-S transect. The Newland transition zone is dominated by silty shales at location 14 (Fig. 2), contains silty shale (minor amounts), carbonaceous swirl shale and striped shale at location 8 and 11 (Fig. 2), is dominated by striped shale at localities 1, 2, 3, 4, 12, and 15 (Fig. 2), and contains only carbonaceous streak shale at location 6 (Fig. 2). This is a proximal-distal arrangement as predicted in Fig. 22.

Facies arrangements in the upper member of the Newland Formation are also as predicted (Fig. 22), because it contains essentially only carbonaceous swirl shale at location 14 (Fig. 2), is strongly dominated by striped shale in the southern Little Belt and northern Big Belt Mountains, and contains about 30-40% carbonaceous streak shale at location 6 (Fig. 2). In the lower member of the Newland Formation carbonaceous streak shale occurs interbedded with gray dolomitic shale at location 6 (Fig. 2), but further north only gray dolomitic shale occurs. This is an arrangement as predicted in Figure 22. Lateral association of gray dolomitic shales, calcareous silty shales, and carbonaceous swirl shales can so far only be inferred from interbedding in shale/carbonate transition zones.

The position of carbonaceous streak shales (continuous sedimentation) basinward of striped shales (Fig. 22) appears incompatible with mainly episodic sedimentation for the striped shales, but can be explained with deposition of carbonaceous streak shales as lateral equivalents of the LaHood Formation. Semiarid climate (Schieber, 1985) would have allowed close association of carbonate producing environments (McMannis, 1963; Boyce, 1975) and terrigenous depocentres in the LaHood Formation, analogous to modern reef-alluvial fan associations (Friedman, 1968). LaHood deltas (Boyce, 1975) may have introduced a continuous (though variable) supply of clay and silt, and offshore mixing of deltaic sediment plumes with carbonate mud and microbial mat fragments (contributed from nearshore productive areas) could upon settling have produced carbonaceous streak shales. This scenario removes the above noted contradiction, and is supported by sole marks marks of sandstone beds in carbonaceous streak shales at location 6 (Fig. 2) that indicate transport from the south (Schieber, 1987). Silt may also have been contributed by aeolian action. My view of shale facies associations, sediment sources, and sedimentary processes is summarized in Fig. 23.

CONCLUSION

Observations made on shale samples from the midProterozoic Newland Formation show that, contrary to popular opinion, shales can reveal a large variety of textural features when studied carefully (Fig. 3). As is possible with carbonates and sandstones, shale facies based on textural features can be defined, and can be recorded during measuring of stratigraphic sections and mapping.

It also becomes clear that shale facies can be interpreted in terms of conditions at the time of deposition (Fig. 23). Interpretation of sedimentary environments of shales is, of course, more tentative than that of carbonates and sandstones where interpretation is facilitated by well known sedimentary structures and by numerous case studies. It stands to reason that, if detailed petrographical and sedimentological studies of shales were as numerous as those conducted on sandstones and carbonates, sedimentologists would have greater confidence to interpret depositional environments of shales. That in turn would yield valuable additional insights into the origin of many sedimentary basins, particularly those that contain large proportions of shales.

ACKNOWLEDGMENTS

I would like to thank Dr G. J. Retallack for helpful discussions concerning the sedimentological aspects of these shales, and Drs N. R. O'Brien, P. E. Potter, and W. A. Pryor for helpful reviews of the manuscript. Field work in Montana was supported by Anaconda Minerals Co.

REFERENCES

AIGNER, T. & REINECK, H.-E. (1982) Proximality trends in modern storm sands from the Helgoland Bight (North Sea) and their implications for basin analysis. *Senckenberg. mar., 14, 183-215.*

BATHURST, R.G.C. *(1972)* Subtidal gelatinous mat, sediment stabilizer and food, Great Bahama Bank. J. *Geol., 75, 736738.*

BOYCE, R.L. (1975) *Depositional systems in the LaHood Formation (Belt Supergroup), southwestern Montana,* unpublished PhD Thesis, University of Texas at Austin, 247 pp.

BROCK, T.D. (1976) Environmental microbiology of living stromatolites. In: *Stromatolites* (Ed. by M. R. Walter). *Developments in Sedimentology, 20,* 141-148, Elsevier, Amsterdam.

BURGER, K. (1963) Kaolin-iibergangstonstein, das genetischfazielle, bilaterale Bindeglied zwischen Kaolin-Kohlentonstein and Kaolin-Pseudomorphosentonstein. *Geol. Mitt., 4,* 115-153.

DoTT, R.H. & BOURGEOIS, J. (1982) Hummocky stratification: Significance of its variable bedding sequences. *Bull. geol. Soe. Am., 93,* 663-680.

FOLK, R.L. (1960) Petrography and origin of the Tuscarora, Rose Hill, and Keefer Formations, Lower and Middle Silurian of eastern West Virginia. *J. sedim. Petrol., 30, 1* 59.

FOLK, R.L. (1962) Petrography and origin of the Silurian Rochester and McKenzie Shales, Morgan County, West Virginia. *J. sedim. Petrol., 32,* 539-578.

FRIEDMAN, G. M. (1968) Geology and geochemistry of reefs, carbonate sediments, and waters, Gulf of Aquaba (Elat), Red Sea. *J. sedim. Petrol., 38,* 895-919.

GEBELEIN, C.D. (1969) Distribution, morphology, and accretion rate of recent subtidal algal stromatolites, Bermuda. *J. sedim. Petrol., 39,* 49-69.

GERDES, G., KRUMBEIN, W.E. & REINECK, H.E. (1985) The depositional record of sandy, versicolored tidal flats (Mellum Island, southern North Sea). *J. sedim. Petrol., 55,* 265-278.

HARMS, J.C., SOUTHARD, J.B., SPEARING, D.R. & WALKER, R.G. (1975) Depositional environments as interpreted from primary sedimentary structures and stratification sequences. Soc. *econ. Paleont. Miner. Short Course Notes, 2,* 161 pp.

HARRISON, J.E. (1972) Precambrian Belt basin of northwestern United States: Its geometry, sedimentation, and copper occurrences. *Bull. geol. Soc. Am., 83,* 1215-1240.

HORODYSKI, R.J. (1980) Middle Proterozoic shale facies microbiota from the lower Belt Supergroup, Little Belt Mts., Montana. *J. Paleont., 54,* 649-663.

LUCIA, F.J. (1972) Recognition of evaporite-carbonate shoreline sedimentation. *Spec. Pubis Soc. econ. Paleont. Miner., Tulsa, 17,* 160-191.

MATTIAT, B. (1969) Eine Methode zur elektronen-mikroskopischen Untersuchung des Microgefuges in tonigen Sedimenten. *Geol. Jahrb., 88,* 87-111.

MCCAVE, I. N. (1970) Deposition of fine-grained suspended sediment from tidal currents. *J. geophys. Res., 75,* 41514159.

MCCAVE, I.N. (1971) Wave effectiveness at the sea bed, and its relationship to bedforms and deposition of mud. *J. sedim. Petrol., 41,* 89-96.

MCMANNIS, W.J. (1963) LaHood Formation-a coarse elastic facies of the Belt Series in southwestern Montana. *Bull. geol. Soc. Am., 74,* 407-436.

MIDDLETON, G.V. & HAMPTON, M.A. (1976) Subaqueous sediment transport and deposition by sediment gravity flows. In: *Marine Sediment Transport and Environmental Management* (Ed. by D. J. Stanley and D. J. P. Swift), pp. 197-218. Wiley, New York.

NELSON, W.H. (1963) Geology of the Duck Creek Pass quadrangle, Montana. *Bull. US geol. Surv.,* ***1121J,*** 56 pp.

NEUMANN, A.C., GEBELEIN, C.D. & SCOFFIN, T.P. (1970) The composition, structure and erodability of subtidal mats, Abaco, Bahamas. *J. sedim. Petrol., 40,* 274-297.

O'BRIEN, N.R. (1970) The fabric of shale-an electronmicroscope study. *Sedimentology,15,* 229-246.

O'BRIEN, N.R. (1980) Use of clay fabric to distinguish turbiditic and hemipelagic siltstones and silts. *Sedimentology, 27,* 47-61.

O'BRIEN, N.R. (1981) SEM study of shale fabric-a review. *Scanning Electron Microscopy,* 569-575.

POTTER, P.E., MAYNARD, J.B. & PRYOR, W.A. (1980) *Sedimentology of Shale.* Springer, New York, 306 pp.

REINECK, H.E. & SINGH, I.B. (1972) Genesis of laminated sand and graded rhythmites in storm-sand layers of shelf mud. *Sedimentology, 18,* 123-128.

REINECK, H.E. & SINGH, I.B. (1980) *Depositional Sedimentary Environments* (2nd edn). Springer, New York, 549 pp.

REINECK, H.E. & WUNDERLICH, F. (1969) Die Entstehung von Schichten and Schichtbanken im Watt. *Senckenberg. mar., 1,* 85-106.

RUBEY, W.W. (1931) Lithologic studies of fine-grained Upper Cretaceous sedimentary rocks of the Black Hills region. US *geol. Surv. Pap., 165A,* 54 pp.

SCHIEBER, J. (1985) *The relationship between basin evolution and genesis of stratiform sulfide horizons in Mid-Proterozoic sediments of Central Montana (Belt Supergroup),* Unpublished PhD Thesis, University of Oregon, 811 pp.

SCHIEBER, J. (1986a) Stratigraphic control of rare-earth pattern types in Mid-Proterozoic sediments of the Belt Supergroup, Montana, U.S.A.: Implications for basin analysis. *Chem. Geol., 54,* 135-148.

SCHIEBER, J. (1986b) The possible role of benthic microbial mats during the formation of carbonaceous shales in shallow Proterozoic basins. *Sedimentology, 33,* 521-536.

SCHIEBER, J. (1987) Storm-dominated epicontinental elastic sedimentation in the Mid-Proterozoic Newland Formation, Montana, USA. N. Jb. *Geol. Paldont. Mh., 27,* 417439.

SEILACHER, A. (1982) Distinctive features of sandy tempestites. In: Cyclic *and Event Stratification* (Ed. by G. Einsele and A. Seilacher), pp. 333-349, Springer, Berlin.

STEWART, J.H. (1976) Late Precambrian evolution of North America: plate tectonics implication. *Geology, 4,* 11-15.

SUNDBORG, A. (1967) Some aspects of fluvial sediments and fluvial morphology. l : General views and graphic methods. *Geograf. Ann., 49,* 333-343.

VON DER BORCH, C.C. (1976) Stratigraphy and formation of Holocene dolomitic carbonate deposits of the Coorong area, South Australia. *J. sedim. Petrol., 46,* 952-966.

WALTHER, J. (1884) *Einleitung in die Geologie als historische Wissenschaft, Bd. 3, Lithogenesis der Gegenwart.* Fischer Verlag, Jena, pp. 535-1055.

WILSON, J.L. (1975) *Carbonate facies in Geologic History.* Springer, New York, 471 pp.

WINDOM, H.L. (1975) Eolian contributions to marine sediments. *J. sedim. Petrol., 45,* 520-529.